Supplementary Information (SI) for Journal of Materials Chemistry C.

Supporting Information

Green Solvent-Free Synthesis of Divinylbenzo[c][1,2,5]thiadiazole Emitters via Hand-Grinding Horner–Wadsworth–Emmons Reaction for High-Performance OLEDs

Premkumar Gnanasekaran[a], Yi-Qi Chao[b‡], Chia-Yu Chen [a], Yi-Ting Chen[b], Jun-Kai Peng[a], Jun-Cheng Lin[c], Chin-Wei Lu[c], Chih-Hao Chang*[b], Yuan Jay Chang*[a]

[a] Department of Chemistry, Tunghai University, Taichung 40704, Taiwan.
[b] Department of Electrical Engineering, Yuan Ze University, Taoyuan 32003, Taiwan;
[c] Department of Applied Chemistry, Providence University, Taichung 43301, Taiwan.
[‡] *Equal contribution first author*

Contents

∗ Corresponding author.

Tel.:+886-3-4638800 ext 7517; fax: + 886-3-4514281;
E-mail address: chc@saturn.yzu.edu.tw (C.-H. Chang)

Tel.: +886-4-23590121 ext 32224; fax: +886-4-23590426;

E-mail address: jaychang@thu.edu.tw (Y. J. Chang)

1. Experimental

All reactions and manipulations were performed under a nitrogen atmosphere unless specified, and solvents were freshly distilled according to standard procedures. The ^{1}H and ^{13}C NMR were recorded on a Bruker AVIII HD 400. The ^{1}H and ^{13}C NMR chemical shifts were reported on δ scale downfield from $(CH_3)_4Si$. The coupling constants (J) were given in hertz. Absorption spectra were recorded on a Shimadzu UV-1800 spectrophotometer, and emission spectra were obtained using a Hitachi F-4500 spectrofluorimeter. Emission spectra in solutions were measured using a spectral grade solvent and right-angle detection. Mass spectra were recorded on a Jeol JMS-700 double-focusing mass spectrometer. Analytical thin layer chromatography (TLC) was performed on Silica gel 60 F 254 Merck. Column chromatography was performed using the silica gel from Merck (Kieselgel Si 60; 40–63 μm). Solvent THF was distilled with sodium benzophenone ketyl. Toluene and dichloromethane were distilled with CaH_2. Other solvents and reagents were reagent grade, purchased from Acros, Alfa, Merck, Lancaster, TCI, Sigma-Aldrich, and Showa, which were directly used without purification.

Fabrication and Characterization of OLEDs: Indium tin oxide (ITO)-coated glass and commercial organic materials were purchased from Lumtec and Shine Materials Technology. Organic materials were subjected to temperature-gradient sublimation in a high vacuum before use. The ITO substrate was washed in sequence with deionized water and acetone, followed by treatment with plasma for 5 minutes. The bottom-emitting OLEDs were fabricated using ITO as the anode, followed by the deposition of multiple organic layers, topped by a metal cathode layer. The organic and metal layers were deposited by thermal evaporation in a vacuum chamber with a base pressure of $< 10^{-6}$ Torr. Device fabrication was completed in a single cycle without breaking the vacuum. The deposition rates of organic materials and aluminum were respectively kept at around 0.1 and 0.5 nm s^{-1}. The active area was defined by the shadow mask (2×2 mm^2). Current density-voltage-luminance characterization was done using two Keysight B2901A current source-measure units equipped with a calibrated Si-photodiode. The electroluminescent spectrum of the devices were recorded using an Ocean Optics spectrometer (Ocean Optics 2000).

Quantum Chemistry Computations: Geometry optimization of the emitters were accomplished by the calculations were performed using the standard 6-31G(d) basis set in Gaussian 16. For excited states, the time-dependent density functional theory (DFT) and the B3LYP functional were used. The frontier orbital plots of the highest occupied molecular orbital (HOMO) and the lowest unoccupied molecular orbital (LUMO) were drawn by using GaussView 06.

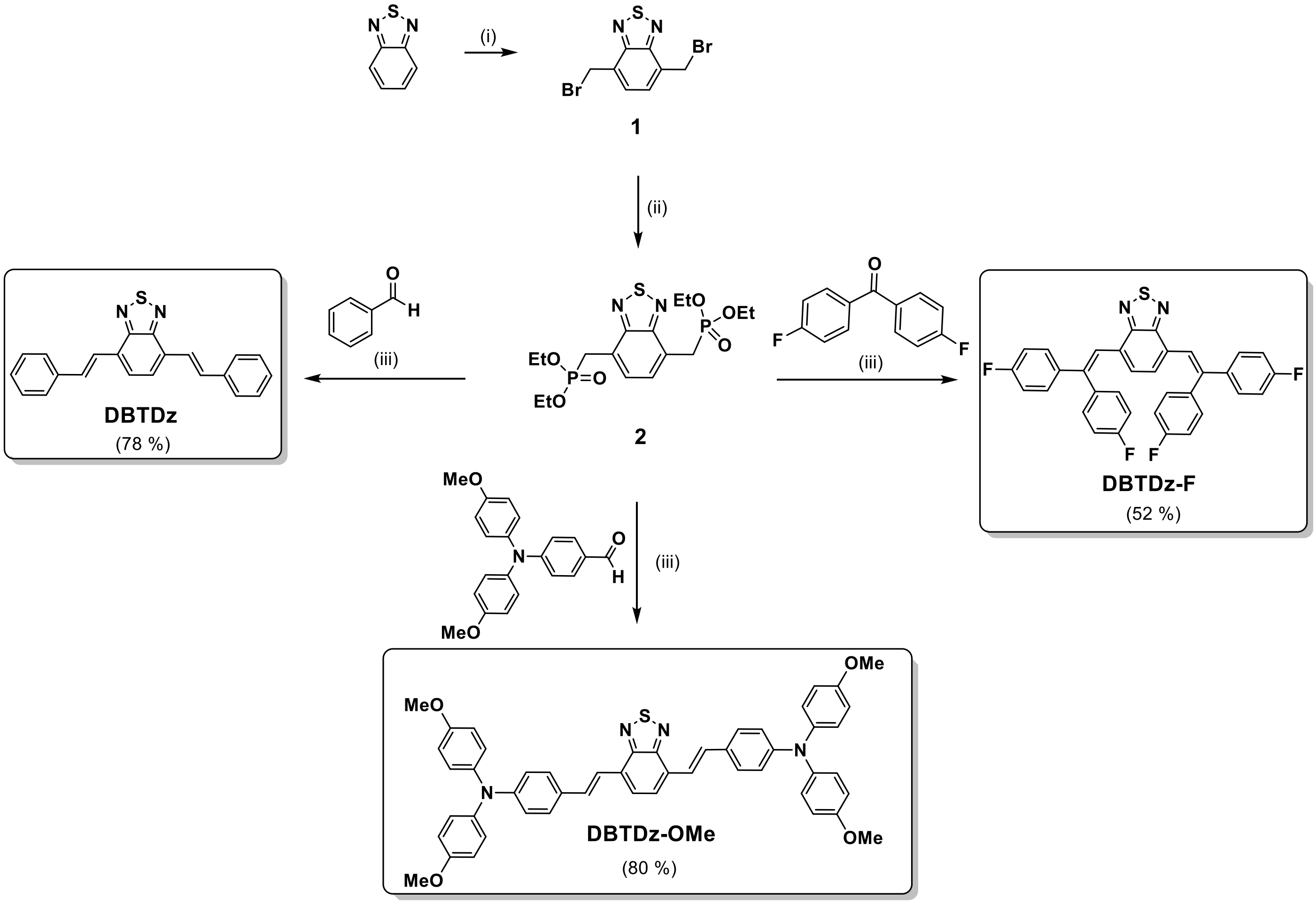

Scheme S1. General synthetic protocol for the synthesis of 4,7 Distyrylbenzo[c][1,2,5]thiadiazole (**DBTDz**) and 4,7-bis(2,2-diphenylvinyl)benzo[c][1,2,5]thiadiazole (**DBTDz-F**) derivatives. Reaction conditions: (i) Trioxane (5 equiv), Tetradecyltrimethylammonium bromide (10 mol%), aqueous HBr, H_2SO_4, reflux, 16 h. (ii) Triethyl phosphite (10 equiv), 150 °C, 24 h. (iii) Benzaldehyde (2.2 equiv), KO^{t}Bu (10 equiv), grinding, RT, 1 min.

Synthesis of 4,7-bis(bromomethyl)benzo[c][1,2,5]thiadiazole (**1**). In a round bottom flask of 500 mL containing 300 mL of HBr and benzo[c][1,2,5]thiadiazole (10 g, 73.437 mmol) was added under slows stirring at room temperature followed by the addition of 1,3,5-trioxane (28.3 ml, 369 mmol) and tetradecyltrimethylammonium bromide (2.47 g, 7.343 mmol) and finally 50 mL of conc. H_2SO_4 was added slowly to the reaction mixture allowed to reflux for 16 hours, after which reaction mixture cooled down to room temperature and nullify with saturated NaOH, extracted with ethyl acetate and concentrated under reduced pressure, afford the off-white precipitate then followed by crystallization in toluene affords the white crystalline powder of 4,7-bis(bromomethyl)benzo[c][1,2,5]thiadiazole (**1**) (17.08 g, 53.5 mmol) in yield of 72 %. Physical appearance: Off-white crystalline solid. R*f* value: 0.51 (Eluent: 10% EA in Hexane). ^{1}H NMR (400 MHz, $CDCl_3$) δ 7.62 (s, 2H), 4.96 (s, 4H). ^{13}C NMR (101 MHz, $CDCl_3$) δ 153.66, 131.33, 129.46, 28.20. MS (HR-FAB): m/z calcd. for $C_8H_6Br_2N_2S$; 319.86, found 320.870 $[M+H]^+$.

Synthesis of tetraethyl(benzo[c][1,2,5]thiadiazole-4,7-diylbis(methylene))bis(phosphonate (**2**). In a 50 mL round bottom flask, 4,7-bis(bromomethyl)benzo[c][1,2,5]thiadiazole (**1**) (1 g, 3.10 mmol). was added and followed by the addition of 10 equivalents of triethyl phosphite (5.33 ml, 31.05 mmol) and allowed to reflux for 24 hours. After that reaction mixture cooled down to room temperature and excess triethyl phosphite was removed under reduced pressure, afford the tetraethyl(benzo[c][1,2,5]thiadiazole-4,7-diylbis(methylene))bis(phosphonate (**2**) (1.16 g, 2.67 mmol) in yield of 86 %. (**2**) (1.16 g, 2.67 mmol) in yield of 86 %. Physical appearance: Colourless liquid. R*f* value: 0.2 (Eluent: 40% EA in Hexane). ^{1}H NMR (400 MHz,) δ 7.55 (s, 2H), 4.02 (p, *J* = 7.0 Hz, 8H), 3.72 (s, 2H), 3.66 (s, 2H), 1.15 (t, *J* = 8.0 Hz, 12H). ^{13}C NMR (101 MHz, $CDCl_3$) δ 154.75, 129.77, 124.16, 124.10, 62.32, 62.29, 62.26, 29.78, 28.39, 16.39, 16.36, 16.33. MS (HR-FAB): m/z calcd. for $C_{16}H_{26}N_2O_6P_2S$; 436.10, found 437.107 $[M+H]^+$.

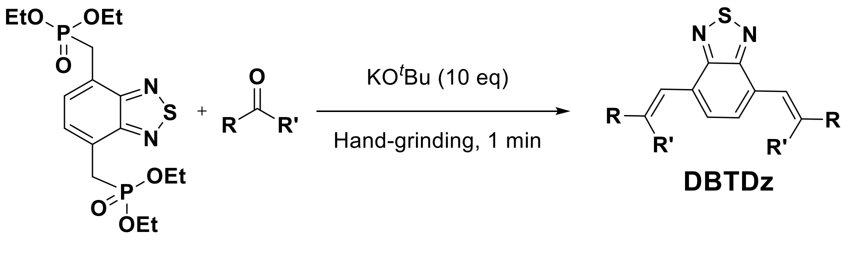

Scheme S2. Synthesis of 4,7-bis(2,2-diphenylvinyl)benzo[c][1,2,5]thiadiazole (**DBTDz**) derivatives. **2** (1 g, 2.29 mmol), carbonyl compound (2.2 equiv, 5.041 mmol), potassium tert-butoxide (2.6 g 22.9 mmol), hand grinding in mortar and pestle in ambient conditions.

*Selected spectral data of the Fluorescent Emitters (**DBTDz**)*

DBTDz: Isolated yield; 78%. Physical appearance: Yellow colour solid. R*f* value: 0.48 (Eluent: 10% EA in Hexane). ^{1}H NMR (400 MHz,) δ 8.01 (s, 1H), 7.97 (s, 1H), 7.65 (m, 8H), 7.41 (t, *J* = 9.0 Hz, 4H), 7.31 (t, *J* = 9.0 Hz, 2H). ^{13}C NMR (101 MHz, $CDCl_3$) δ 153.93, 137.48, 133.20, 129.33, 128.77, 128.17, 126.93, 124.48. MS (HR-FAB): m/z calcd. for $C_{22}H_{16}N_2S$; 340.10, found 340.103 [M^+].

DBTDz-F: Isolated yield; 52%. Physical appearance: Orange colour solid. R*f* value: 0.51 (Eluent: 15% EA in Hexane). ^{1}H NMR (400 MHz, $CDCl_3$) δ 7.60 (s, 2H), 7.36 – 7.30 (m, 4H), 7.16 – 7.11 (m, 4H), 7.06 – 6.96 (m, 8H), 6.63 (s, 2H). ^{13}C NMR (101 MHz, $CDCl_3$) δ 154.90, 143.51, 138.90, 132.05, 131.97, 129.71, 129.63, 128.89, 127.93, 122.49, 116.13, 115.92, 115.52, 115.30. ^{19}F NMR (376 MHz, $CDCl_3$) δ -113.51 – -113.59 (m, 2F), -113.59 – -113.69 (m, 2F). MS (HR-FAB): m/z calcd. for $C_{34}H_{20}F_4N_2S$; 564.13, found 564.128 [M^+].

DBTDz-OMe: Isolated yield; 80%. Physical appearance: Dark-brown colour solid. R*f* value: 0.4 (Eluent: 10% EA in Hexane). ^{1}H NMR (400 MHz, $CDCl_3$) δ 7.89 (s, 1H), 7.85 (s, 1H), 7.61 (s, 2H), 7.51 (s, 1H), 7.45 (d, *J* = 8.8 Hz, 5H), 7.09 (d, *J* = 8.8 Hz, 8H), 6.93 (d, *J* = 8.5 Hz, 4H), 6.85 (d, *J* = 8.8 Hz, 8H), 3.81 (s, 12H). ^{13}C NMR (101 MHz, $CDCl_3$) δ 156.16, 154.12, 148.83, 140.69, 132.52, 129.79, 129.26, 127.79, 126.93, 126.28, 121.92, 120.27, 114.85, 55.63. MS (HR-FAB): m/z calcd. for $C_{50}H_{42}N_4O_4S$; 794.29, found 794.293 [M^+].

2. ^{1}H and ^{13}C NMR spectra

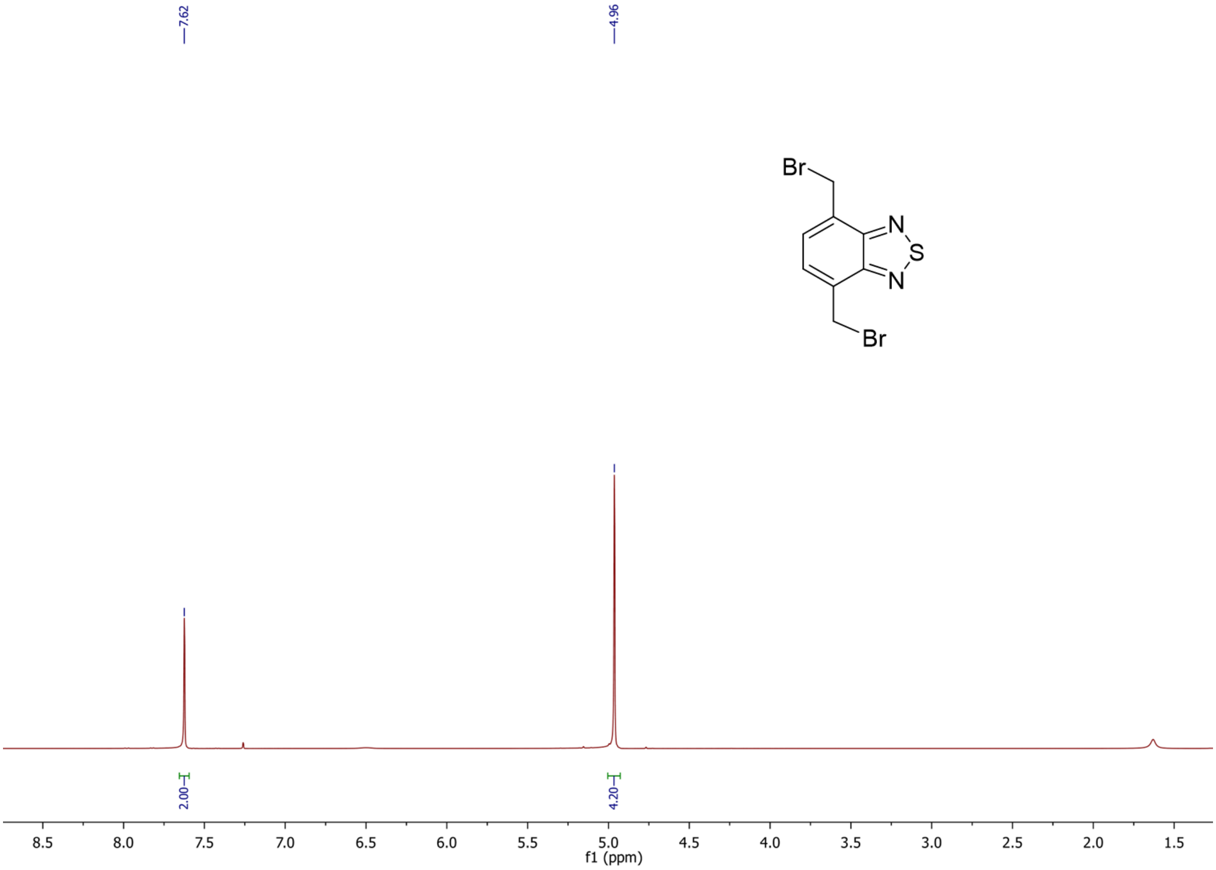

Fig. S1. ^{1}H NMR (up) spectrum of **1**.

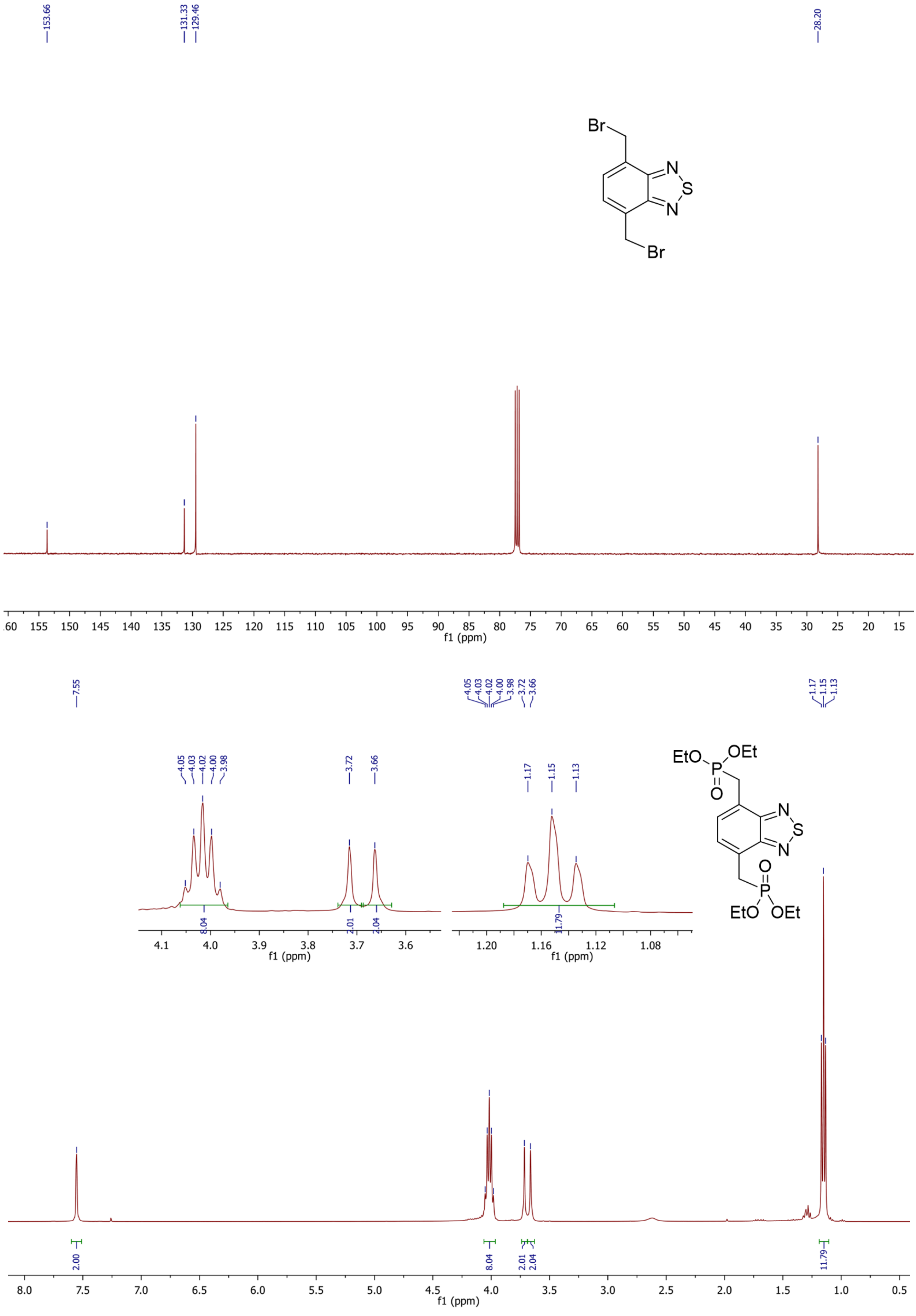

Fig. S2. ^{13}C NMR (up) spectrum of **1**, ^{1}H NMR (down) spectrum of **2**.

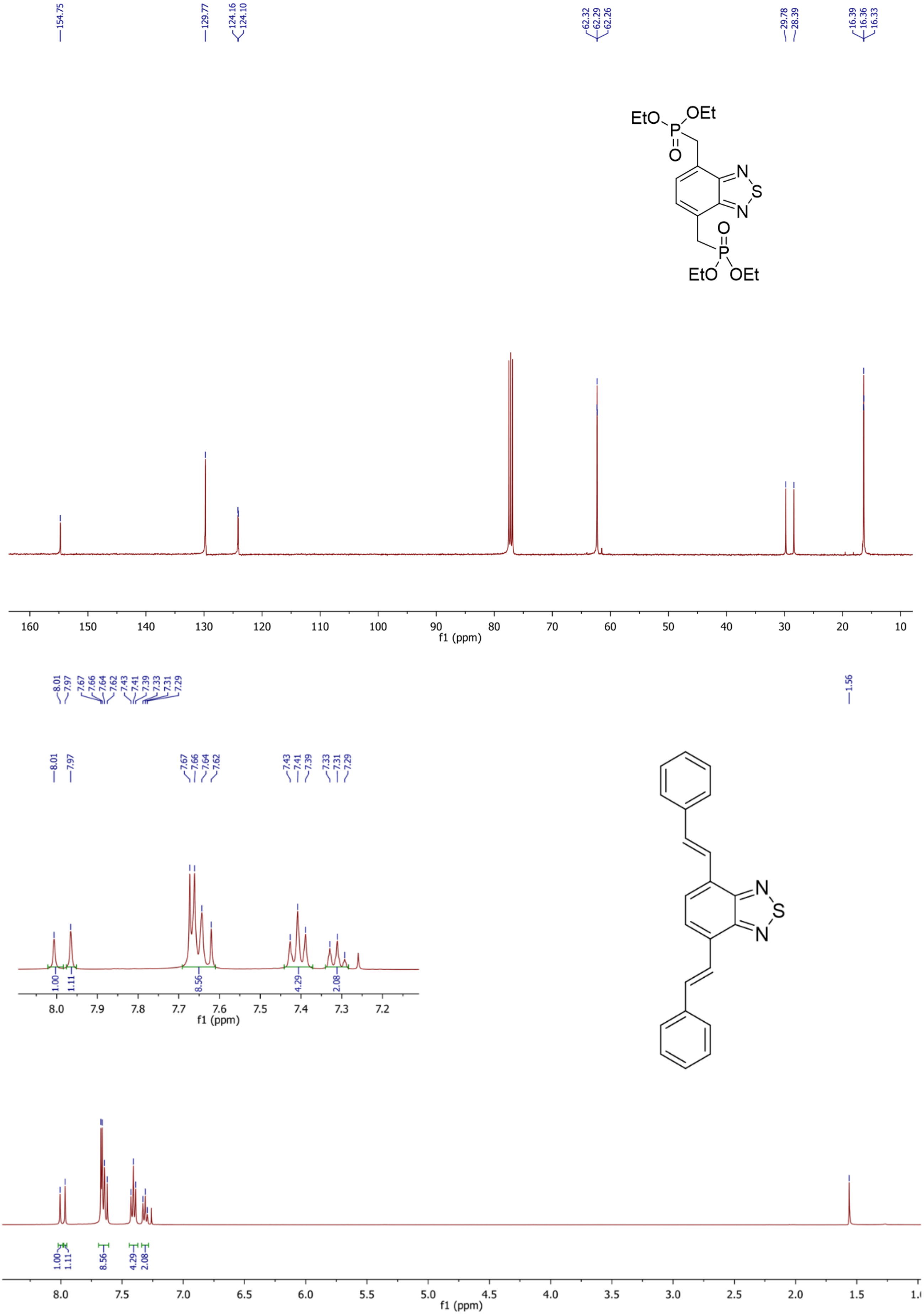

Fig. S3. ^{13}C NMR (up) spectrum of **2**, ^{1}H NMR (down) spectrum of **DBTDz**.

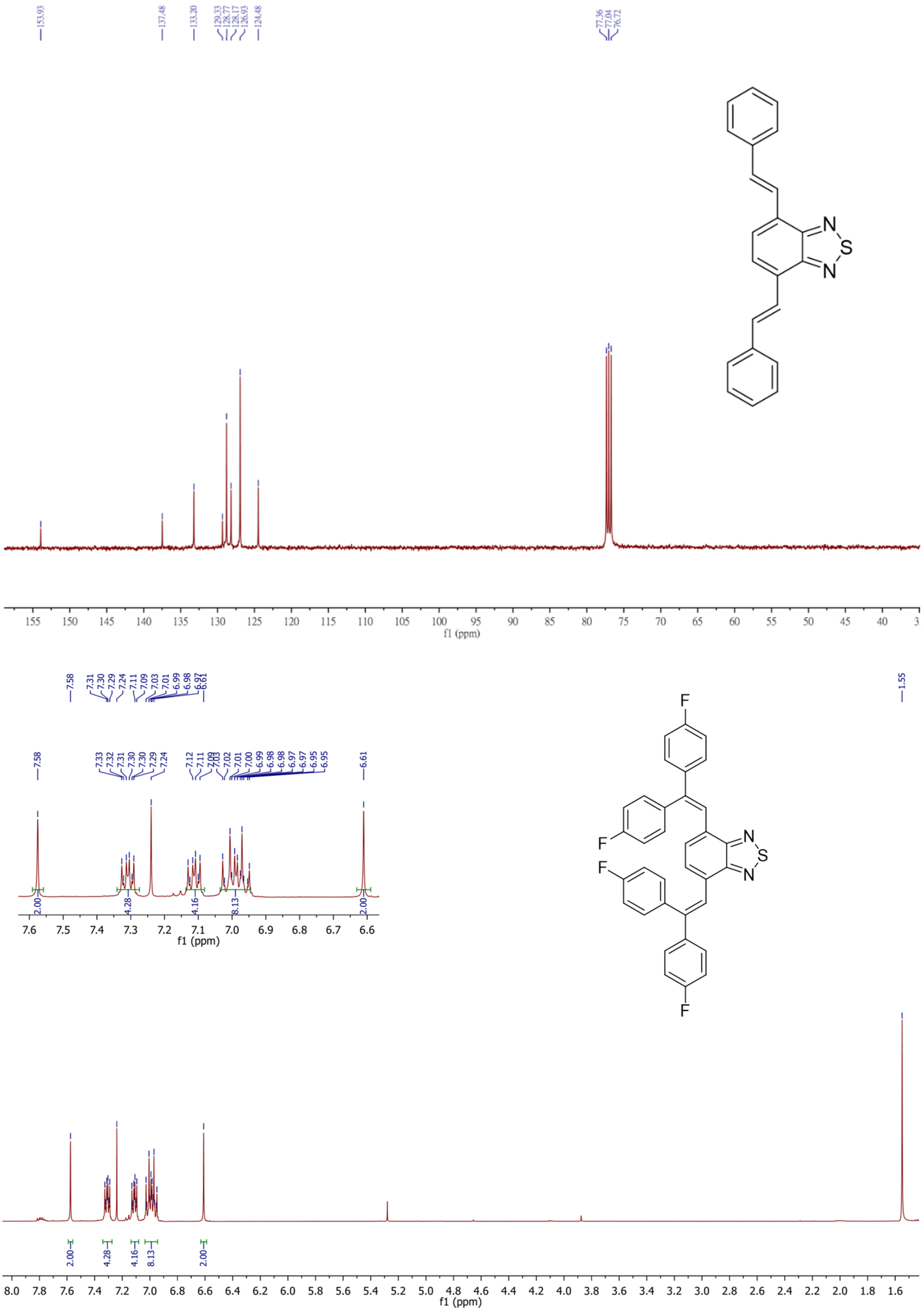

Fig. S4. ^{13}C NMR (up) spectrum of **DBTDz**, ^{1}H NMR (down) spectrum of **DBTDz-F**.

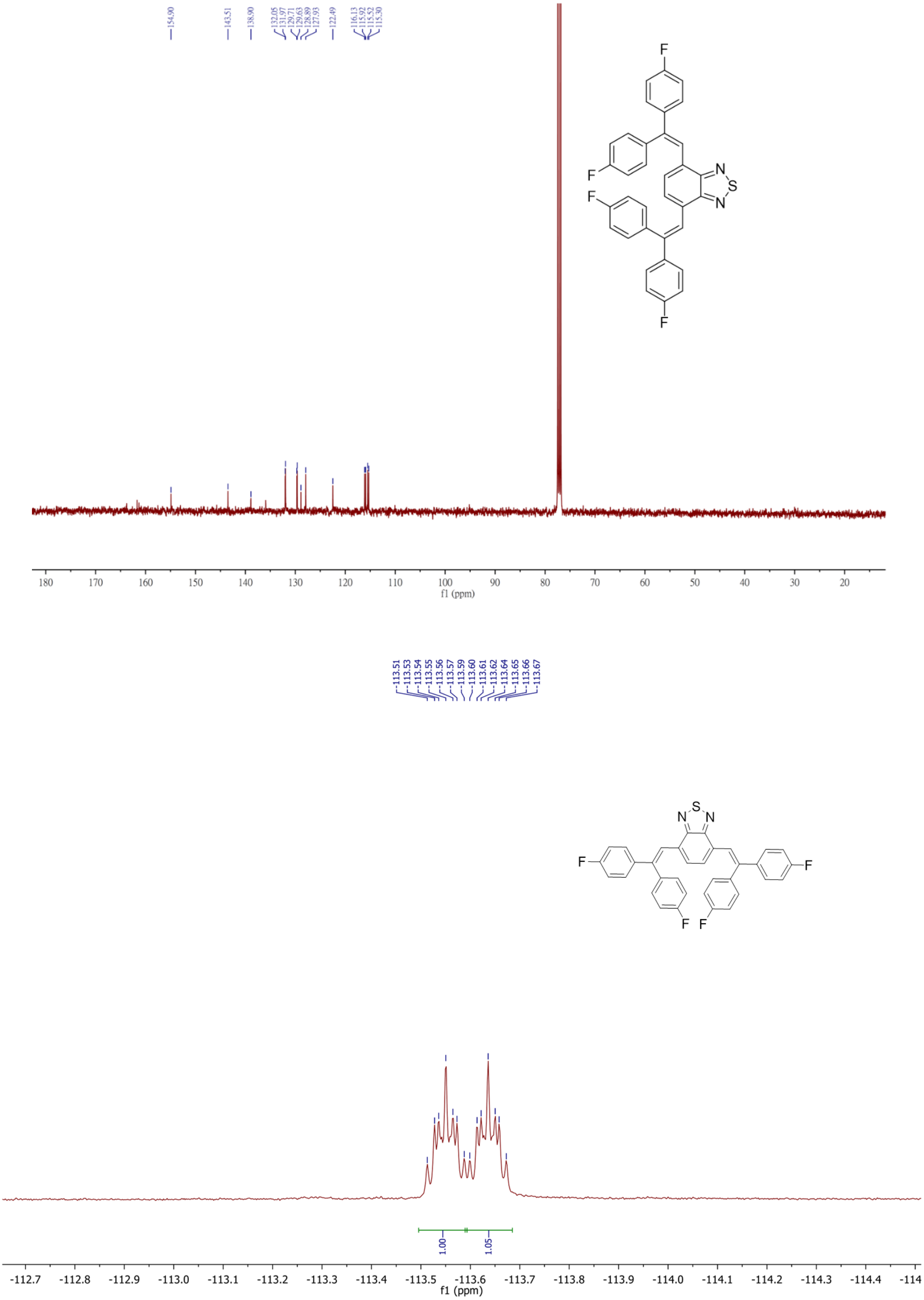

Fig. S5. ^{13}C NMR (up), ^{19}F NMR (down) spectrum of **DBTDz-F**.

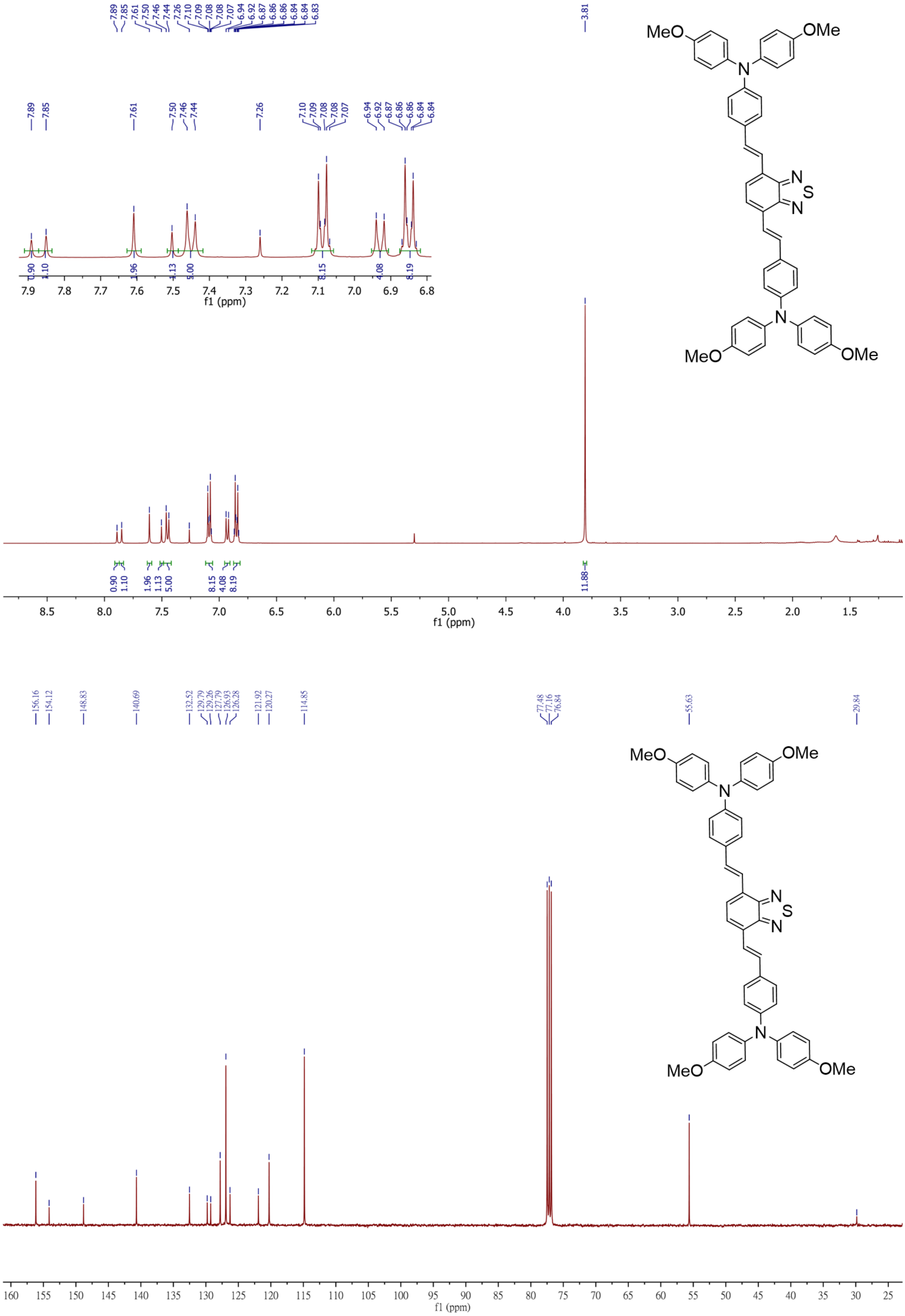

Fig. S6. ^{1}H NMR (up) ^{13}C NMR spectrum of **DBTDz-OMe**.

3. Theoretical calculation

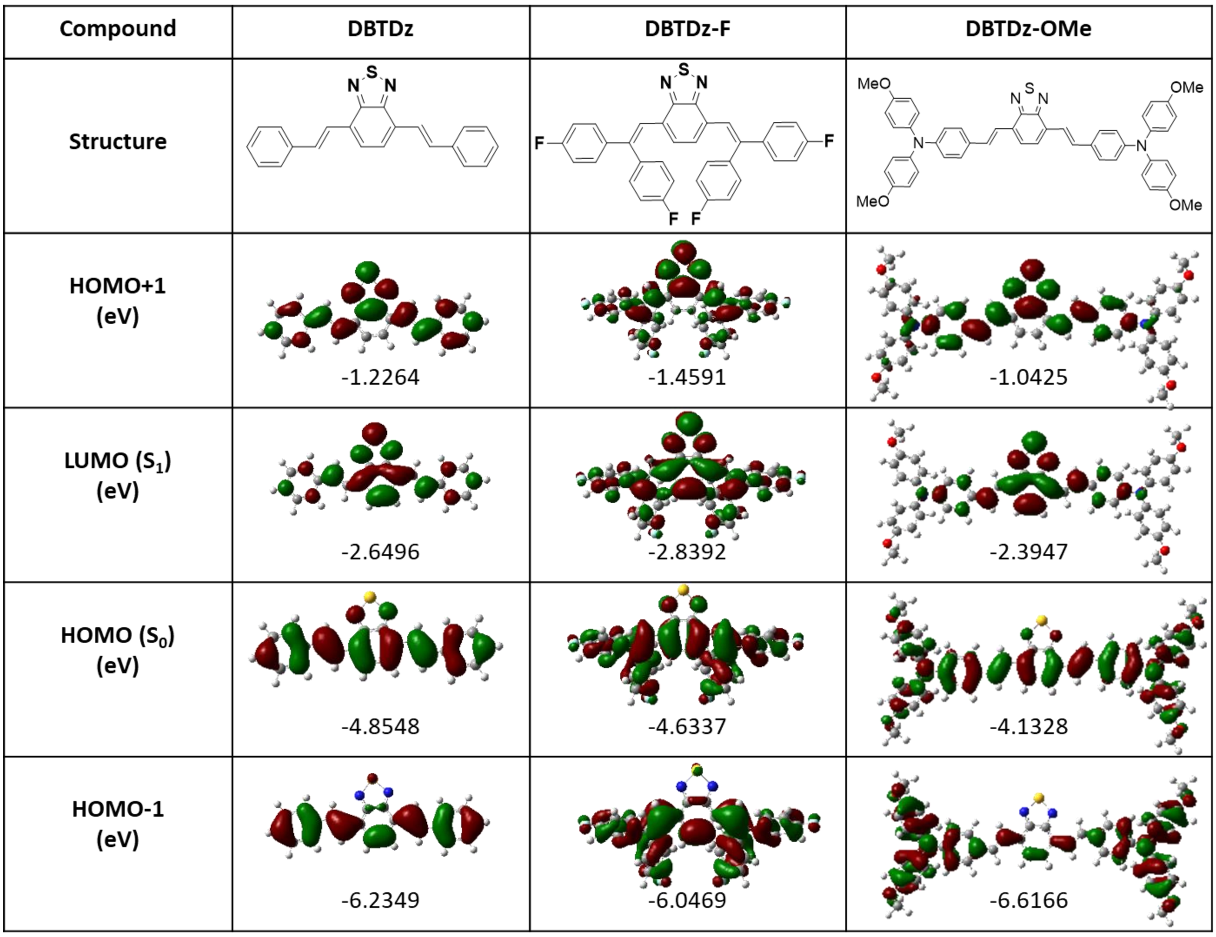

Compound	DBTDz	DBTDz-F	DBTDz-OMe
Structure			
HOMO+1 (eV)	-1.2264	-1.4591	-1.0425
LUMO (S_1) (eV)	-2.6496	-2.8392	-2.3947
HOMO (S_0) (eV)	-4.8548	-4.6337	-4.1328
HOMO-1 (eV)	-6.2349	-6.0469	-6.6166

Fig. S7. HOMO/LUMO levels of **DBTDz**-based emitters.

Table S1. Theoretically calculated energy level of first excited triplet state (T_1), HOMO-LUMO energy gap (E_g), and singlet-triplet energy difference (ΔE_{ST}) of **DBTDz** fluorescent emitters.

Compound	S_0 (eV)	S_1 (eV)	E_g (eV)	T_1 (eV)	ΔE_{ST} (eV)	$\Delta E_{S0\text{-}T1}$ (eV)
DBTDz	-4.8548	-2.6496	2.2052	-3.8446	1.195	1.0102
DBTDz-F	-4.6337	-2.8392	-1.7945	-3.9658	1.126	0.6679
DBTDz-OMe	-4.1328	-2.3947	-1.7381	-3.2158	0.8211	0.917

Table S2. Theoretically calculated electronic transitions and dipole moments of **DBTDz** fluorescent emitters.

	state	**Excitation**	***f*cal (eV, nm)**	***f* B3LYP/6-31G***	**Dipole moment (Debye)**
DBTDz	S1	HOMO → LUMO 89 ->90 69.302%	2.0317, 610.25	0.5777	1.1878
	S2	HOMO-1 → LUMO 88 -> 90 65.207%	3.1517, 393.38	0.0251	
	S3	HOMO → LUMO +1 89 -> 91 66.976%	3.2862, 377.29	1.2791	
DBTDz-F	S1	HOMO → LUMO 145 ->146 70.727%	1.6035, 773.23	0.4516	0.8424
	S2	HOMO-1 → LUMO 144 ->146 61.834%	2.6786, 462.88	0.0077	
	S3	HOMO → LUMO+1 145 ->147 69.526%	2.6900, 460.91	0.3519	
DBTDz-OMe	S1	HOMO → LUMO 209 -> 210 70.409%	1.5470, 801.43	1.1710	1.3208
	S2	HOMO-1 → LUMO 208 ->210 70.054%	2.0139, 615.66	0.0089	
	S3	HOMO-2 → LUMO 207 ->210 65.601%	2.5402, 488.09	0.0682	

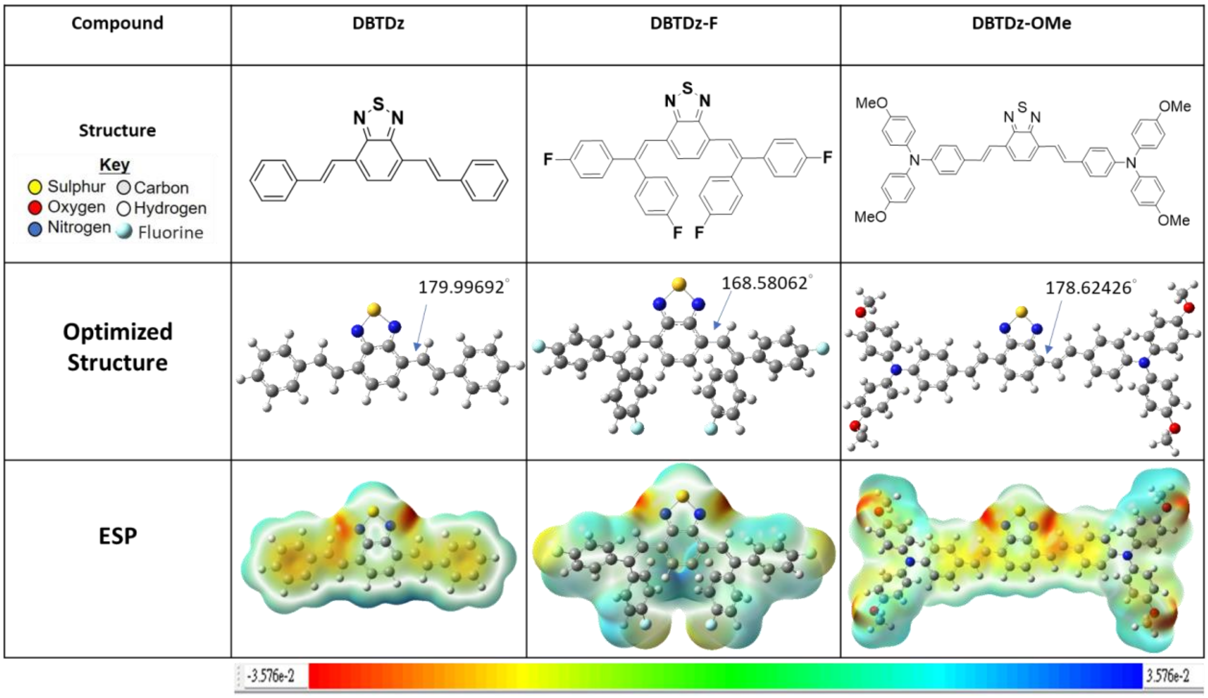

Fig. S8. Theoretically optimized structures, dihedral angles, and ESP maps of **DBTDz** emitters.

4. Photoluminescenes characteristic of the florescent emitters

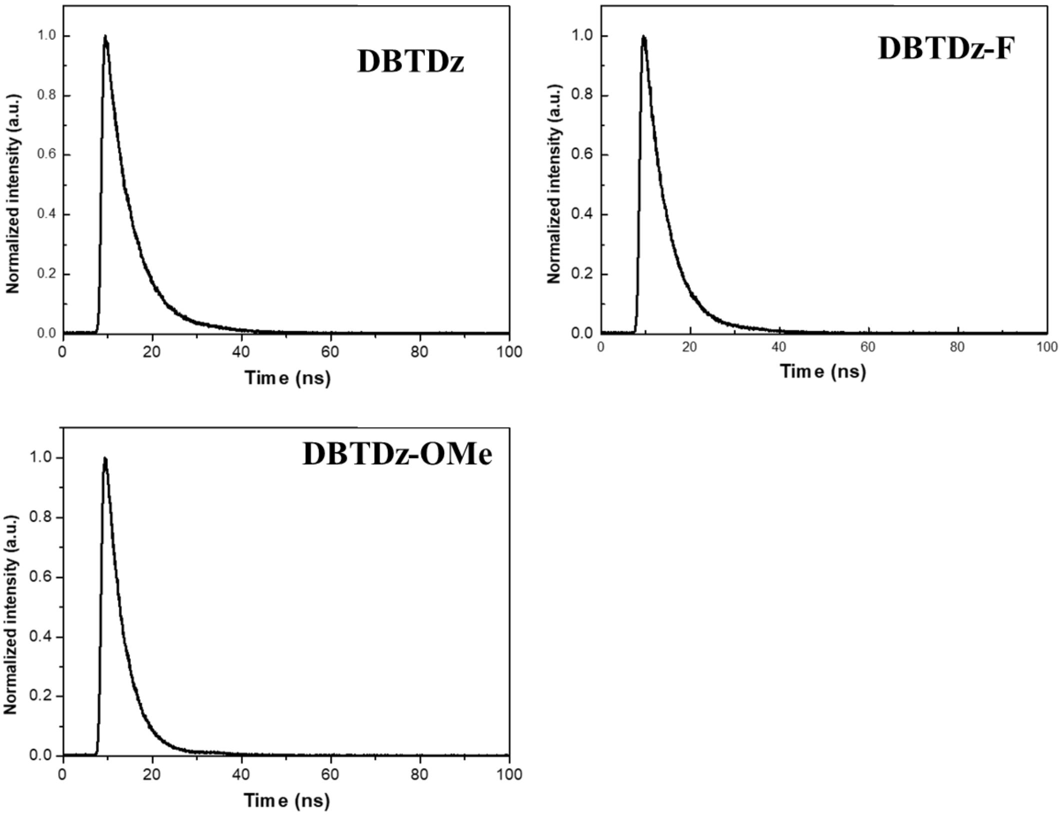

Fig. S9. Transient PL decay of the **DBTDz**, **DBTDz-F** and **DBTDz-OMe** fluorescent emitters.

5. Single-crystal X-ray diffraction Analysis

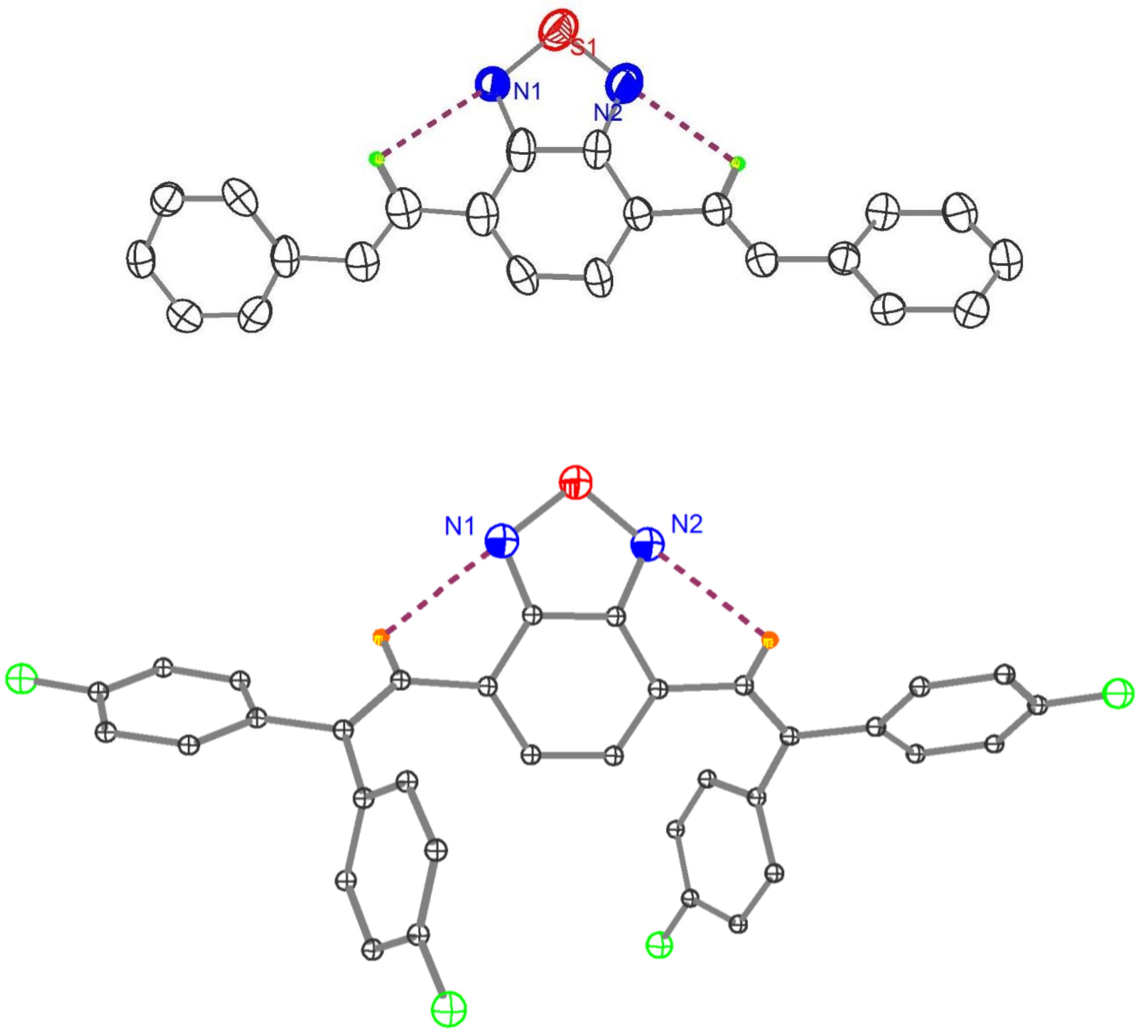

Fig. S10. Single crystal structure of **DBTDz** (up) and **DBTDz-F** (down).

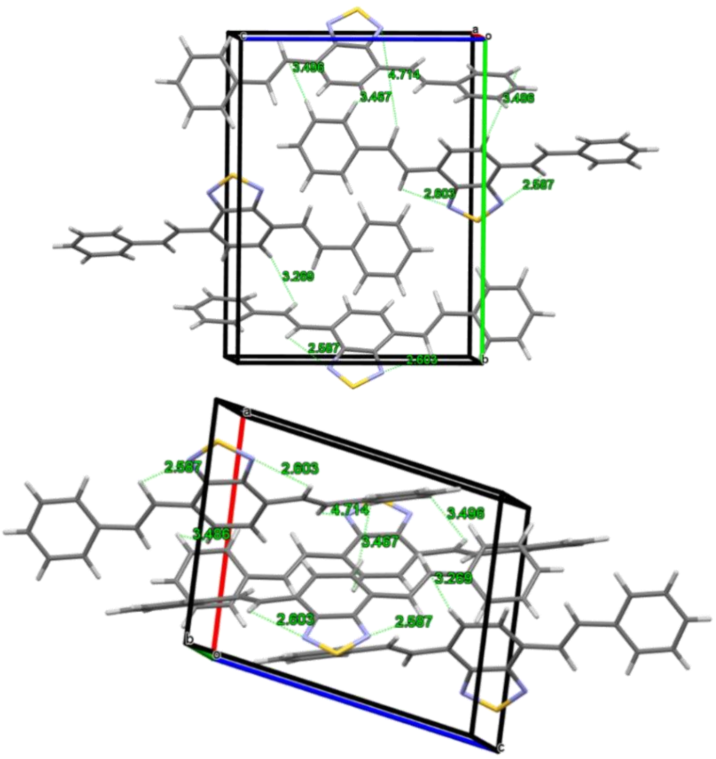

Fig. S11. Crystal packing of **DBTDz** with different view angles. The distance between the molecular fragments is indicated by a green dashed line.

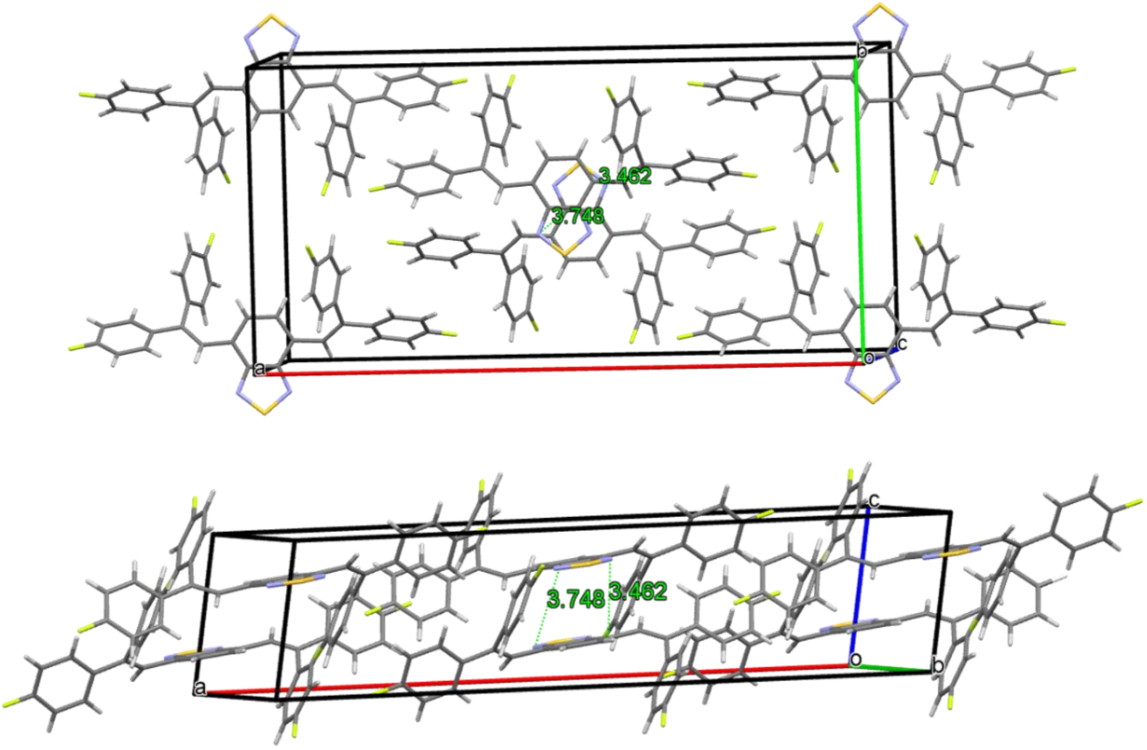

Fig. S12. Crystal packing of **DBTDz-F** with different view angles. The distance between the molecular fragments is indicated by a green dashed line.

Table S3. Crystal data and structure refinement for DBTDz and DBTDz-F fluorescent emitters.

Identification Code	DBTDz (CCDC 2474743)	DBTDz-F (CCDC 2474744)
Empirical formula	$C_{22}H_{16}N_2S$	$C_{34}H_{20}F_4N_2S$
Formula weight	340.43	564.58
Temperature	150.15 K	150(2) K
Wavelength	0.71076 Å	0.71073 Å
Crystal system	Monoclinic	Monoclinic
Space group	P121/c 1	C2/c
Unit cell dimensions	a = 9.5987(5) Å	a = 29.3094(12) Å
	α= 90°.	α= 90°.
	b = 15.0870(9) Å	b = 14.7807(7) Å
	β= 101.039(2)°.	β= 98.9151(7)°.
	c = 11.7651(7) Å γ = 90°.	c = 6.9665(3) Å γ = 90°.
Volume	1672.25(17) Å^3	2981.5(2) Å^3
Z	4	4
Density (calculated)	1.352 mg/m^3	1.258 mg/m^3
Absorption coefficient	0.200 mm^{-1}	0.158 mm^{-1}
F(000)	712	1160
Crystal size	? x ? x ? mm^3	0.450 x 0.130 x 0.110 mm^3
Theta range for data collection	2.549 to 26.390°.	2.756 to 27.899°.
Index ranges	-11<=h<=11, -18<=k<=18, -14<=l<=14	-38<=h<=38, -19<=k<=19, -9<=l<=8
Reflections collected	50871	34377
Independent reflections	3404 [R(int) = 0.0600]	3562 [R(int) = 0.0348]
Completeness to theta = 25.242°	99.6 %	99.7 %

Absorption correction	None	Semi-empirical from equivalents
Max. and min. transmitttion	0.7455 and 0.6667	0.7455 and 0.6667
Refinement method	Full-matrix least-squares on F^2	Full-matrix least-squares on F^2
Data / restraints / parameters	3404 / 1 / 282	3562 / 1 / 186
Goodness-of-fit on F^2	1.041	1.000
Final R indices [I>2sigma(I)]	R1 = 0.0878, wR2 = 0.2208	R1 = 0.0510, wR2 = 0.1532
R indices (all data)	R1 = 0.1206, wR2 = 0.2716	R1 = 0.0595, wR2 = 0.1643
Extinction coefficient	n/a	n/a
Largest diff. peak and hole	1.426 and -1.122 e.Å^{-3}	0.506 and -0.569 e.Å^{-3}

6. Cyclic voltammetry (CV) spectroscopy

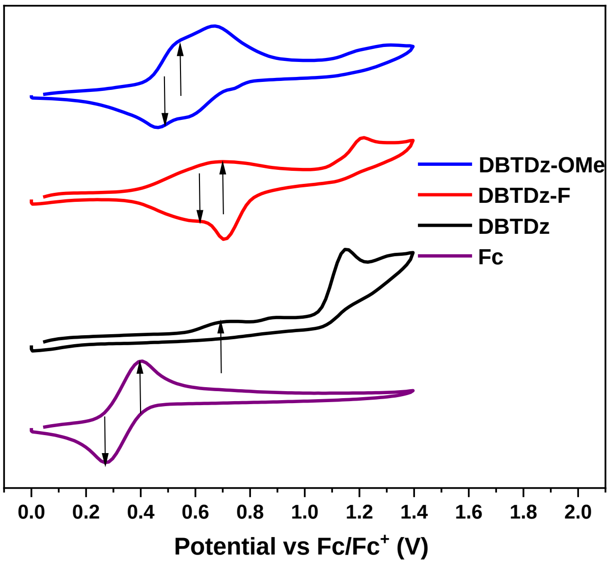

Fig. S13. Cyclic voltammograms of **DBTDz**, **DBTDz-F**, and **DBTDz-OMe**. The oxidation potential was measured in CH_2Cl_2 solution at room temperature.

7. Differential scanning calorimetry (DSC) curves

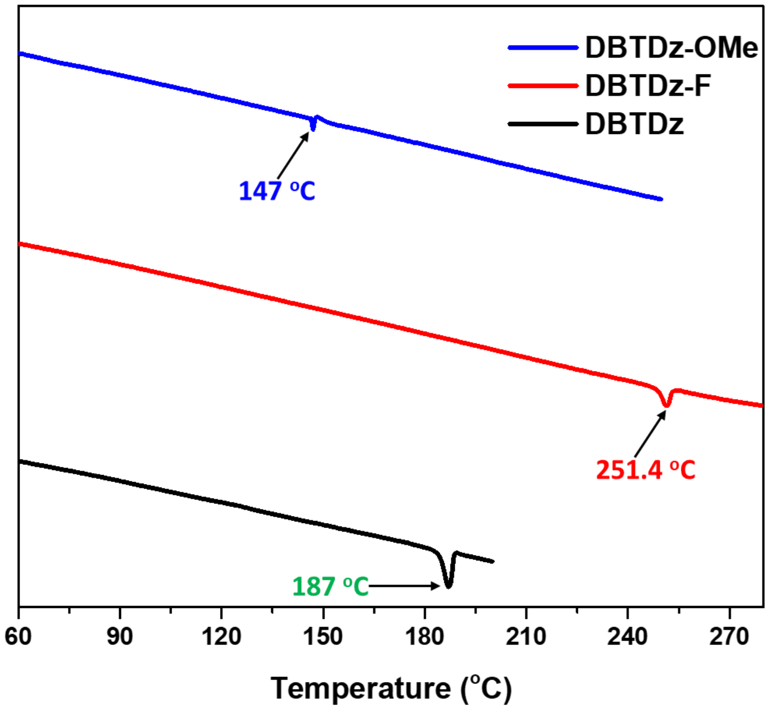

Fig. S14. Differential scanning calorimetry (DSC) curves of **DBTDz** fluorescent emitters.

8. Thermogravimetric analysis (TGA) curves

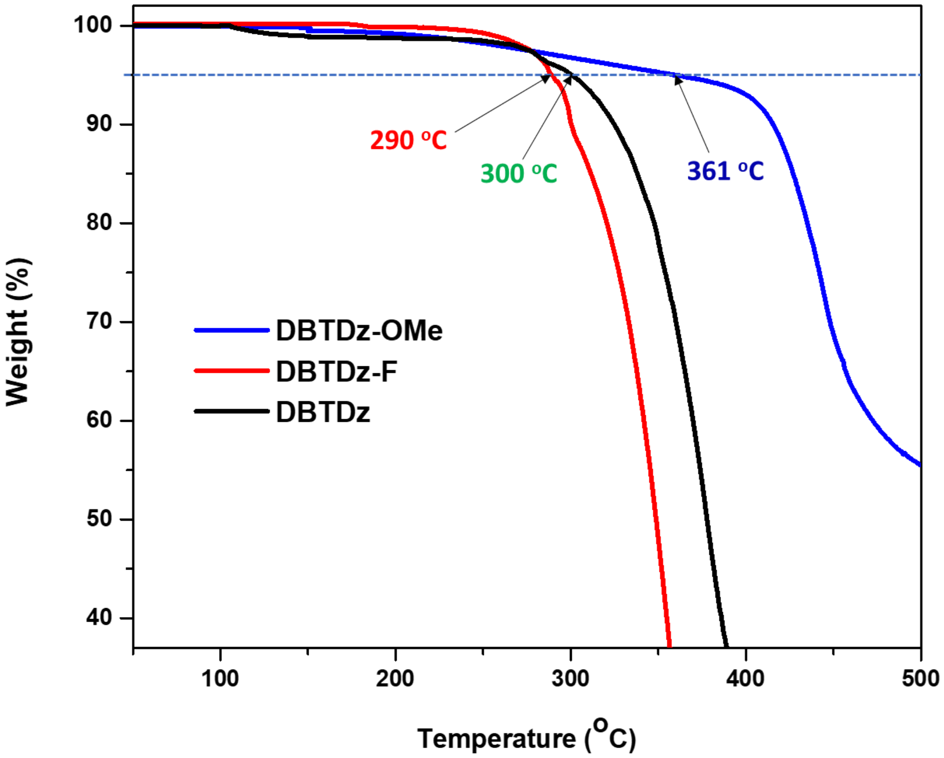

Fig. S15. Thermogravimetric analysis (TGA) curves of **DBTDz**-based emitters.

9. PL spectrum and transient PL decay

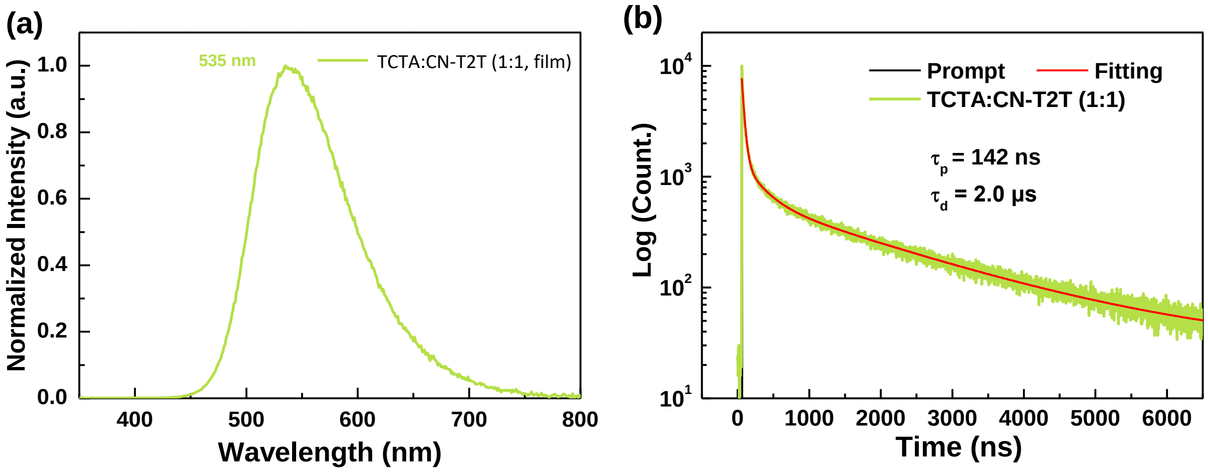

Fig. S16. Thin film sample TCTA:CN-T2T (1:1): (a) PL spectrum of the exciplex emission; (b) transient PL decay.

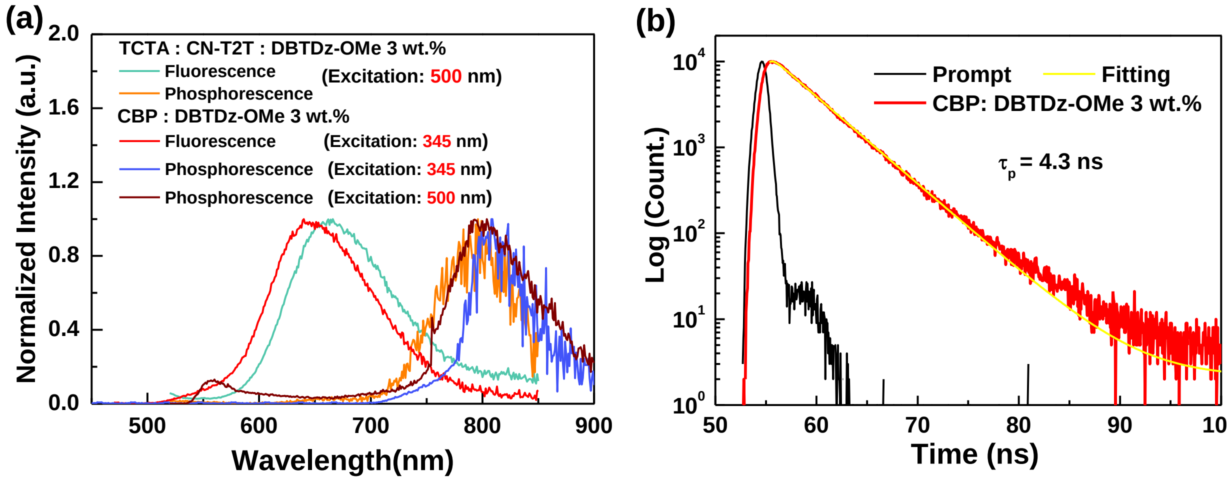

Fig. S17. Fluorescence and phosphorescence spectra of the doped-film samples: TCTA:CN-T2T (1:1): **DBTDz-OMe** 3 wt.% and CBP: **DBTDz-OMe** 3 wt.%. (a) PL spectrum; (b) Transient PL decay curve.